Original Article

Sulfuretted hydrogen ameliorates high dose glucose-induced podocyte apoptosis via orchestrating AMPK/mTOR cascade-mediated anti-apoptotic effects

Yong Huang[1], Jie Cheng[2], Yehua Zhou[2], Yanhui Zhang[2], Shuhui Zhou[2], Qingzhen Li[1], Lin Peng[1], Maohong Wang[1], Weiguo Song[1], Guoqing Wu[1]

[1]Department of Nephrology, Affiliated Hospital of Jiangxi University of Traditional Chinese Medicine, Nanchang, China; [2]Department of Nephrology, Jiangxi University of Traditional Chinese Medicine, Nanchang, China

Contributions: (I) Conception and design: Y Huang, G Wu; (II) Administrative support: J Cheng, Q Li; (III) Provision of study materials or patients: Y Zhou, Y Zhang, M Wang; (IV) Collection and assembly of data: Y Huang, J Cheng, S Zhou, Q Li, L Peng, W Song; (V) Data analysis and interpretation: Y Huang, J Cheng, G Wu; (VI) Manuscript writing: All authors; (VII) Final approval of manuscript: All authors.

Correspondence to: Guoqing Wu, MD. Department of Nephrology, Affiliated Hospital of Jiangxi University of Traditional Chinese Medicine, 445 Bayi Avenue, Donghu District, Nanchang 330006, China. Email: wgq86362665@126.com.

Background: Podocytes play a pivotal role in the glomerular filtration barrier and contribute to proteinuria and glomerulosclerosis through abnormal apoptosis. Longitudinal studies have indicated the protective properties of hydrogen sulfide (H_2S) against neuronal cell apoptosis, whereas the biological function and the underlying molecular mechanism on glucose-induced podocyte apoptosis are largely unknown.

Methods: Herein, we conducted multifaceted biological analyses to verify the potential function of H_2S in glucose-induced podocyte apoptosis by examining apoptotic proteins and markers (e.g., caspase 3, Hoechst) and antioxidative effects [e.g., reactive oxygen species (ROS), lipid peroxidation, superoxide dismutase (SOD), catalase (CAT)]. Then, we took advantage of transcriptome sequencing and biological analyses to further determine the potential influence of H_2S as well as the accompanying molecular mechanism.

Results: In this study, we found that glucose-induced podocyte apoptosis could be largely rescued by H_2S via antioxidative responses, which was further confirmed by transcriptome sequencing and bioinformatics analyses. According to apoptotic signaling analysis, the over-activated AMPK/mTOR signaling cascade in glucose-treated podocytes was effectively restrained.

Conclusions: For the first time, we indicated the protective effect and mechanism of H_2S in podocytes by restricting glucose-induced apoptosis and suppressing the abnormally activated AMPK/mTOR signaling cascade. Our findings provide new references for podocyte apoptosis-associated diseases and also indicate the potential of H_2S administration in clinical trials.

Keywords: Podocyte injury; sulfuretted hydrogen; glucose-induced apoptosis; AMPK/mTOR; reactive oxygen species (ROS)

Submitted Aug 31, 2021. Accepted for publication Oct 20, 2021.
doi: 10.21037/atm-21-5152
View this article at: https://dx.doi.org/10.21037/atm-21-5152

Introduction

Podocytes are glomerular visceral epithelial cells, which together with the glomerular basement membrane, glomerular endothelial cells, surface proteoglycans, and podocyte subregions of endothelial cells, constitute the glomerular filtration barrier (1,2). Podocytes play a pivotal role in the maintenance of the glomerular filtration barrier, whereas podocyte injury usually results in proteinuria and detachment from the human glomerular basement membrane (3,4). Current studies

on the biology and gene disruption of podocytes have indicated the causal relationship between abnormalities of podocytes and proteinuria and glomerulosclerosis (4-6). Over the decades, a number of glomerular responses to podocyte dysfunction have been determined, which has helped to decode the complex scenario of podocyte injury and the resultant consequences. For instance, Dai *et al.* and Li *et al.* found that diabetic nephropathy was associated with functional and morphological alterations of podocytes such as epithelial-mesenchymal transition (EMT), podocyte detachment, podocyte hypertrophy, and podocyte apoptosis (7,8).

Meanwhile, we and other investigators have explored potential therapeutics for podocyte injury and the underlying molecular mechanisms (1,7,8). For example, Egerman and colleagues recently verified the role of plasmin-induced podocyte injury in the puromycin aminonucleoside (PAN) nephropathy model, and have demonstrated that amiloride also has podocyte-protective properties (5). Chen *et al.* verified that hydrogen sulfide (H_2S) confers a protective effect against TNF-α-induced neuronal cell apoptosis via miR-485-5p and type 1-associated DEATH domain protein (TRADD) signaling (9). Also, Liu and colleagues found that H_2S could efficiently reduce neuronal cell apoptosis in a rat spinal cord ischemia-reperfusion injury model by upregulating lncRNA CASC7 (10). Notably, the study by Liu *et al.* indicated the impact of H_2S upon high glucose-induced mouse podocyte injury as well as the underlying mechanisms via ZO-2 upregulation and the suppression of Wnt/β-catenin pathway (11). To date, H_2S has been recognized as a novel gaseous mediator and acts as a neuromodulator and neuroprotective agent in clinical practice (12). However, the effects of exogenous H_2S on podocyte injury, and in particular, glucose-induced podocyte apoptosis, are largely unknown.

In this study, we identified for the first time the protective effects of H_2S on glucose-induced apoptosis of podocytes via inhibiting AMPK/mTOR signaling. In particular, the over-activation of reactive oxygen species (ROS) caused by low or high doses of glucose could be largely rescued by H_2S. In addition, with the aid of RNA-Seq and multifaceted bioinformatics analyses, our study systematically revealed the similarities and variations of differentially expressed genes (DEGs) and the genetic variation spectrum in podocytes with glucose and H_2S treatment. We present the following article in accordance with the MDAR reporting checklist (available at https://dx.doi.org/10.21037/atm-21-5152).

Methods

Cell culture

Rat podocytes (Fenghui, China) were cultured in DMEM basal medium (Procell, China) supplemented with 10% fetal bovine serum (FBS) (Gibco, USA) at 37 ℃ and 5% CO_2. In the experimental groups, podocytes were treated with low D-glucose (LG, 5.5 mmol/L, Procell, China), high D-glucose (HG, 33 mmol/L, Procell, China), and high glucose and sulfuretted hydrogen (HS, 1.0 mM, Sigma, USA).

Flow cytometry (FCM) assay

FCM was conducted as previously described with several modifications (13). In detail, podocytes with the aforementioned treatments were dissociated into single cells and labeled with the indicated antibodies including Annexin-V and 7AAD in 0.2% BSA for 30 min in the dark. Afterwards, the cells were washed with 1× PBS twice and analyzed by FACS Canto II (BD Biosciences, USA). The antibodies are listed in Table S1.

Western blotting

Western blotting analyses were conducted as previously reported (14). In brief, the cell samples at indicated time points were lysed with Laemmli sample buffer (BioRed, USA) and inactivated. After that, the samples were electrophoresed in SDS-PAGE gel (Instant SDS-PAGE Gel, China) and transferred onto a PVDF membrane (Life Sciences, USA). Then, the membrane was incubated with the primary and secondary antibodies after blocking. The detection of the indicated proteins in the samples was accomplished by utilizing the Super-signal West Pico Chemiluminescent Substrate (Prierce, USA) system. The information of the listed antibodies is shown in Table S1.

Enzyme-linked immunosorbent assay (ELISA)

The detection of secreted cytokines in the supernatant was accomplished using ELISA kits (NeoBioscience, China) according to the manufacturer's instructions.

Cell proliferation-associated Cell Counting Kit-8 (CCK-8) analysis

The quantification of podocyte proliferation was performed using the CCK-8 (Dojindo, Japan) according to the manufacturer's instructions. In detail, the population doubling (Pd) curve was generated using standard methods as previously described (15).

Superoxide dismutase (SOD) and catalase (CAT) assay

SOD and CAT were measured using the SOD kit (Jiancheng A001-3, China) and the CAT kit (Jiancheng A007-1-1, China) according to the manufacturer's instructions, respectively. The inhibition ratio of SOD was calculated according to the formula: inhibition ratio of SOD (%) = $[(A_{control} - A_{blank\ of\ control}) - (A_{measure} - A_{blank\ of\ measure})]/(A_{control} - A_{blank\ of\ control}) \times 100\%$. The activity of SOD was calculated according to the formula: activity of SOD (U/mL) = inhibition ratio of SOD/50% × dilution ratio × (0.24 mL/0.02 mL) × sample dilution ratio. The activity of CAT was calculated according to the formula: activity of CAT (U/mL) = $(OD_{control} - OD_{measure}) \times 271 \times [1/(60 \times \text{sample volume})] \times$ sample dilution ratio.

Immunofluorescence staining

The immunofluorescence staining of apoptotic podocytes with the indicated treatments (LG, HG, HS) at the indicated time points (24 and 48 h) was conducted with the Hoechst staining kit (Haoxin Bio-tech, China) according to the manufacturer's instructions. In detail, the podocytes were treated with 70% (v/v) ethanol for 5 min and washed with 1× PBS 3 times. After that, the cells were fixed with 4% polyoxymethylene (Sigma-Aldrich, USA) and stained with the dyeing working fluid for 10 min. Finally, the morphology of the podocytes was observed and recorded under a fluorescence microscope (Laite, USA).

RNA-Seq and bioinformatics analyses

Podocytes at the indicated time points were lysed using the TRIzol reagent (ThermoFisher, USA) for total RNA collection as previously described according to the manufacturer's instructions (15). The total RNA was quantified using NanoDrop 2000 (ThermoFisher), and RNA-Seq was performed using the Beijing Genomics Institute (BGI, China). Bioinformatics analyses were conducted as previously described by utilizing online websites and software (15).

Statistical analysis

The statistical analysis was conducted with Prism 6.0 (GraphPad Software, USA) as previously reported (16,17). A statistically significant difference was considered when the P value was less than 0.05. The data was shown as mean ± SEM (n=3 independent experiments). *, P<0.05; **, P<0.01; ***, P<0.0001; ****, P<0.0001; NS, not significant.

Results

Sulfuretted hydrogen showed protective effects on the apoptosis of podocytes

We found that podocytes with LG or HG stimulation showed characteristics of apoptosis in a dose-dependent and time-dependent manner (*Figure 1A*). Interestingly, the pro-apoptotic effect of glucose treatment could be largely alleviated according to the quantification of caspase 3 activity (*Figure 1A*). To further evaluate the anti-apoptotic effect of sulfuretted hydrogen, we performed Hoechst staining and found that podocytes with high glucose treatment at 48 h showed a higher percentage of apoptotic cells, which could be effectively suppressed by sulfuretted hydrogen (*Figure 1B*). Furthermore, with the aid of FCM, the anti-apoptotic effect of sulfuretted hydrogen in podocytes was also confirmed (*Figure 1C,1D*). Taken together, sulfuretted hydrogen showed protective effects on the apoptosis of podocytes caused by glucose stimulation.

The pro-apoptotic effect of high-dose glucose was effectively rescued by sulfuretted hydrogen

To further explore the protective effect of sulfuretted hydrogen on glucose stimulation-induced apoptosis, we detected the principle pro-apoptotic (e.g., Bax, caspase 3) and anti-apoptotic (e.g., Bcl-2) proteins among the indicated groups. Distinguished from the higher levels of Bax and caspase 3 in the HG group, the HS groups revealed lower levels of pro-apoptotic protein expression, with higher Bcl-2 expression instead (*Figure 1E,1F*). Quantification of apoptosis-associated proteins by gray scanning showed that the HG group manifested the highest levels of Bax and caspase 3, while the HS group had the highest level of Bcl-2 expression (Figure S1).

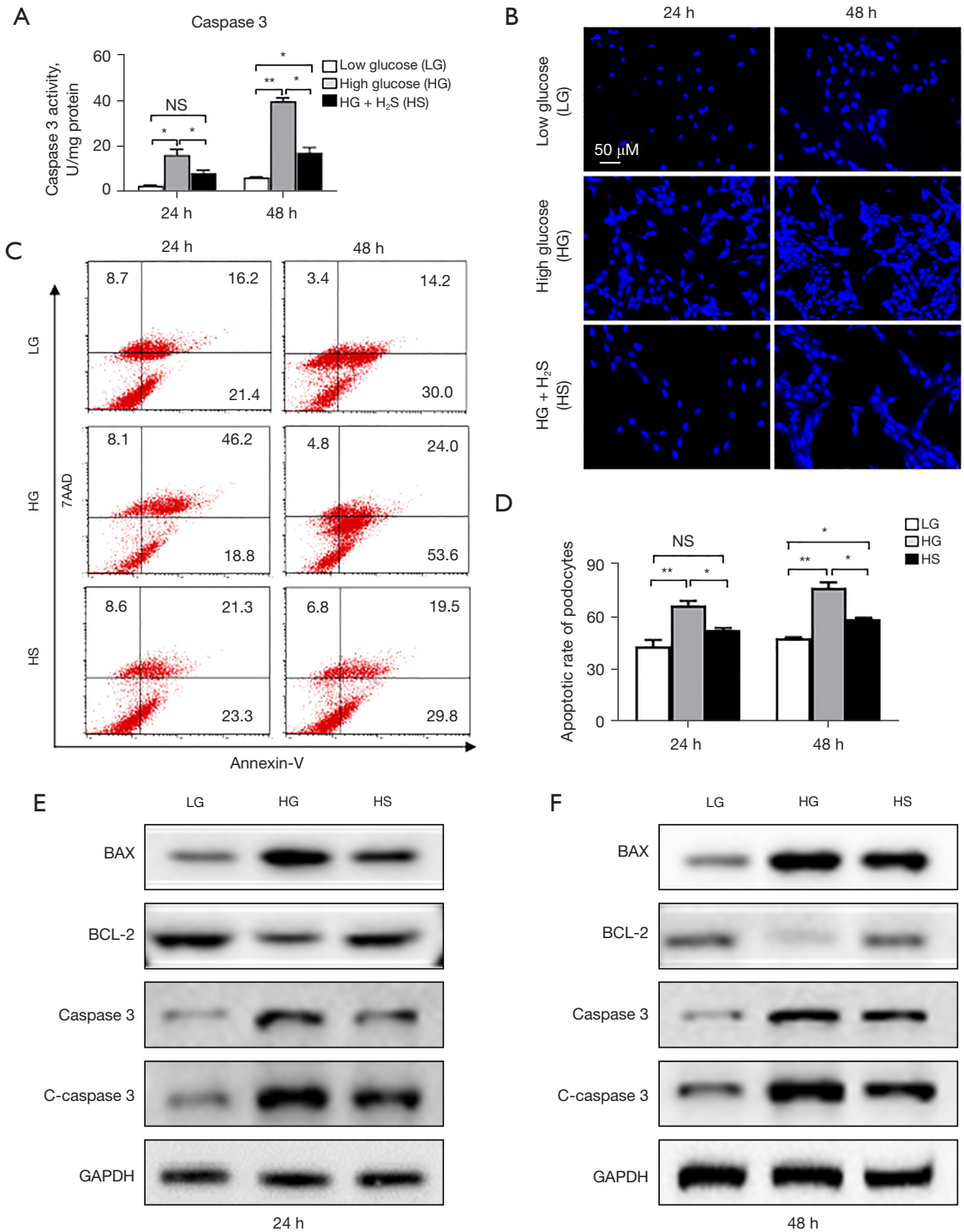

Figure 1 Sulfuretted hydrogen showed protective effects on glucose-induced podocyte apoptosis. (A) Caspase 3 activity in podocytes with LG or HG glucose treatment, or HG and HS treatment at indicated time points (24 and 48 h). All data are shown as mean ± SD (n=3). *, P<0.05; **, P<0.01; NS, not significant. (B) Immunostaining of Hoechst-positive apoptotic podocytes with the indicated treatments. Scale bar =50 μm. (C,D) Representative diagrams (C) and statistical analysis (D) of apoptotic podocytes by the FCM assay. All data are shown as mean ± SD (n=3). *, P<0.05; **, P<0.01; NS, not significant. (E,F) Western blotting analysis of pro-apoptotic (Bax, caspase 3) proteins and anti-apoptotic (Bcl-2) proteins in podocytes with the indicated treatments at 24 h (E) and 48 h (F). GAPDH was the loading control. All data are shown as mean ± SEM (n=3). LG, low D-glucose; HG, high D-glucose; HS, high glucose and sulfuretted hydrogen; FCM, flow cytometry; H_2S, hydrogen sulfide.

The DEGs in podocytes with sulfuretted hydrogen treatment were involved in apoptosis

Having clarified the anti-apoptotic effect at the cellular level, we were curious about the potential influence of sulfuretted hydrogen at the molecular level. To this end, we harvested podocyte samples after glucose and/or sulfuretted hydrogen treatment (LG, HG, HS) at the indicated time points (24 and 48 h), including LG-24 h (LG-24 h-1, LG-24 h-2, LG-24 h-3), HG-24 h (HG-24 h-1, HG-24 h-2, HG-24 h-3), HS-24 h (HS-24 h-1, HS-24 h-2, HS-24 h-3), LG-48 h (LG-48 h-1, LG-48 h-2, LG-48 h-3), HG-48 h (HG-48 h-1, HG-48 h-2, HG-48 h-3), and HS-48 h (HS-48 h-1, HS-48 h-2, HS-48 h-3). With the aid of RNA-Seq, we found that the aforementioned groups showed conservation in the general gene expression profiling based on the reads per kilobase per million (RPKM) values (*Figure 2A*). According to the Venn diagrams, we visually observed the DEGs [|log2(fold change)|>1, P<0.05] among the indicated groups at 24 and 48 h (*Figure 2B,2C*), which were further confirmed by the heatmaps (*Figure 2D*). Furthermore, by utilizing gene ontology (GO) analysis, we verified that the DEGs between the HG-24 h and HS-24 h group were involved in diverse biological processes (BP). For instance, the DEGs at 24 h were concerned with apoptosis, microRNAs in cancer, ubiquitin mediated proteolysis, RNA transport, and protein processing, while those at 48 h were involved in apoptosis, p53 signaling pathway, microRNAs in cancer, and extracellular matrix (ECM)-receptor interaction (*Figure 2E,2F*). Notably, the aforementioned DEGs showed a consistent correlation with apoptosis (*Figure 2E,2F*), which further suggested the anti-apoptotic effect of sulfuretted hydrogen against glucose stimulation at the molecular level.

Podocytes with sulfuretted hydrogen treatment revealed distinguishable signatures of the genetic variation spectrum

Aiming to evaluate the potential influence of sulfuretted hydrogen treatment on podocytes with glucose stimulation, we turned to analyze the signatures of the genetic variation spectrum among the abovementioned groups. By utilizing principal component analysis (PCA), we clearly verified that podocytes with the indicated treatment at the indicated time points revealed distinguishable clusters, while duplicate samples with more similarities in signatures of the genetic variation spectrum were clustered instead (*Figure 3A*). This was further confirmed by variable splice event (VSE) analysis including alternative 3' splicing site (A3SS), alternative 5' splicing site (A5SS), mutually exclusive exon (MXE), retained intron (RI), and skipped exon (SE) (*Figure 3B*). Furthermore, the general information of the somatic variations in podocytes with the indicated treatments were displayed by Circos software, such as the expression and loci regional distribution in the chromosome (*Figure 3C*). Similarly, by conducting GO analysis, we found that the genes with genetic variations between the HG and HS groups at 24 or 48 h were largely involved in the regulation of apoptotic processes, response to hypoxia and hydrogen peroxide, mRNA splicing, regulation of transcription, and protein transport (*Figure 3D,3E*). Taken together, different from those with glucose treatment, podocytes with sulfuretted hydrogen treatment revealed distinguishable signatures of the genetic variation spectrum, and in particular, apoptosis and hypoxia-associated BP.

Sulfuretted hydrogen treatment showed antioxidative protective effects on podocytes

Having uncovered the genetic characteristics among the LG, HG, and HS groups, we questioned the potential influence of sulfuretted hydrogen on the glucose-induced apoptosis of podocytes. Based on the bioinformatics analysis, we explored the protective effects of sulfuretted hydrogen through antioxidative responses. We detected the contents of ROS in podocytes, and found that the level of ROS in the HS groups (HS-24 h, HS-48 h) sharply declined compared with that in the HG groups (HG-24 h, HG-48 h) (*Figure 4A,4B*). Simultaneously, quantification of lipid peroxidation among the indicated groups revealed that malondialdehyde (MDA), the natural product of lipid peroxidation which is involved in oxidative stress, was upregulated in the HG groups and downregulated in the LG and HS groups at 48 h (*Figure 4C*), which collectively indicated the lower level of lipid peroxidation in the latter groups (LG, HS). Inversely, the activity of SOD, an antioxidant metalloenzyme which catalyzes the disproportionation of superoxide anion radicals to oxygen and hydrogen peroxide, was lower in the HG group compared with that in the other groups, while there were no visible differences in the activity of CAT (*Figure 4D,4E*). Collectively, these data further confirmed the protective effects of sulfuretted hydrogen on podocytes via an antioxidant approach.

AMPK/mTOR signaling mediated the anti-apoptotic effect of sulfuretted hydrogen

Current research has indicated the involvement of

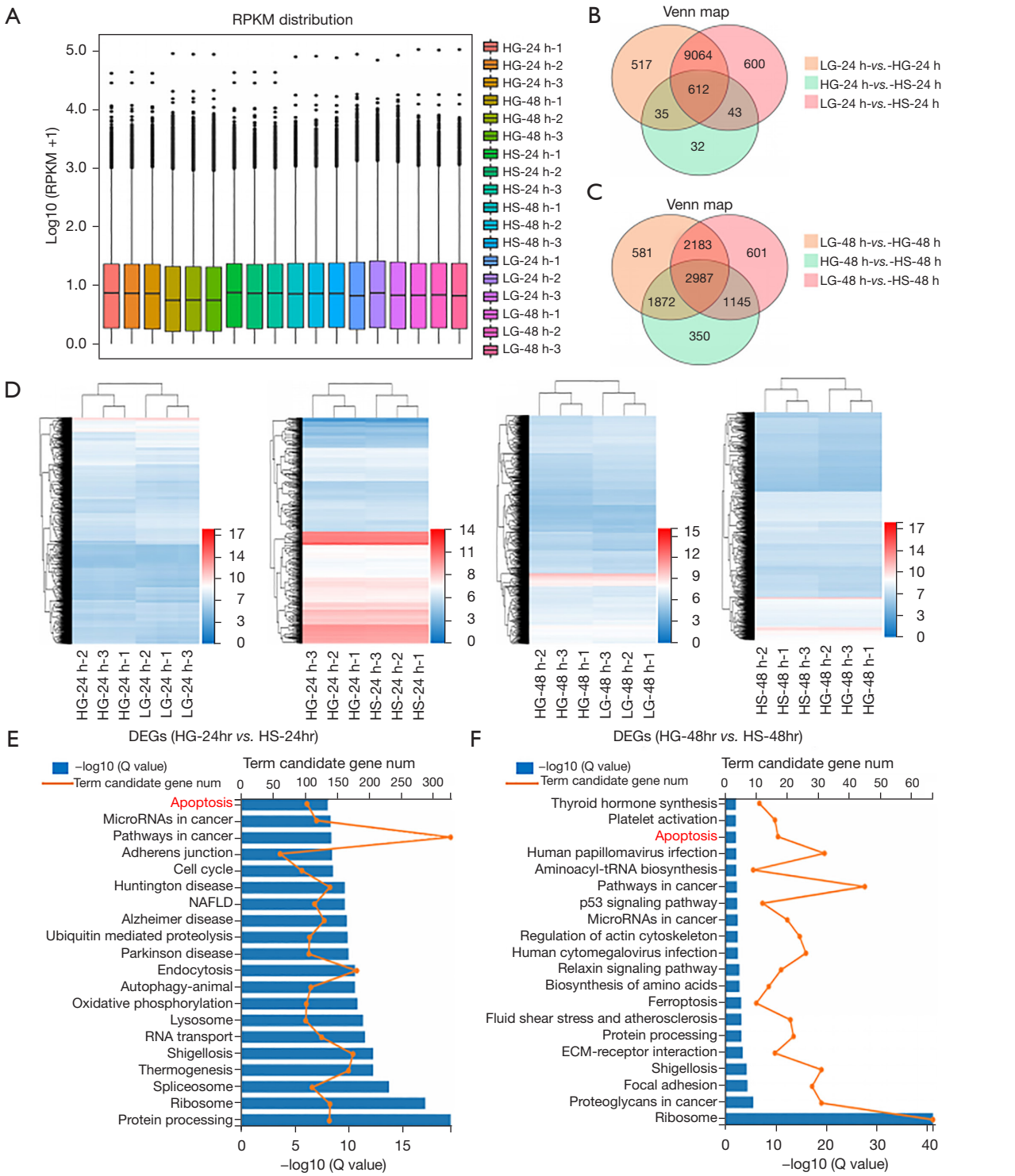

Figure 2 Gene expression profiling of podocytes in the indicated groups. (A) The distribution of gene expression in LG-24 h, HG-24 h, HS-24 h, LG-48 h, HG-48 h, and HS-48 h based on log2 (RPKM +1). (B,C) Venn diagram analysis of DEGs among the indicated groups at 24 h (B) and 48 h (C). (D) Correlation analysis of LG-24 h, HG-24 h, HS-24 h, LG-48 h, HG-48 h, HS-48 h using heatmaps. (E,F) GO analysis of DEGs between HG-24 h and HS-24 h (E), or between HG-48 h and HS-48 h (F). LG, low D-glucose; HG, high D-glucose; HS, high glucose and sulfuretted hydrogen; RPKM, reads per kilobase per million; DEGs, differentially expressed genes; GO, gene ontology; NAFLD, nonalcoholic fatty liver disease; ECM, extracellular matrix.

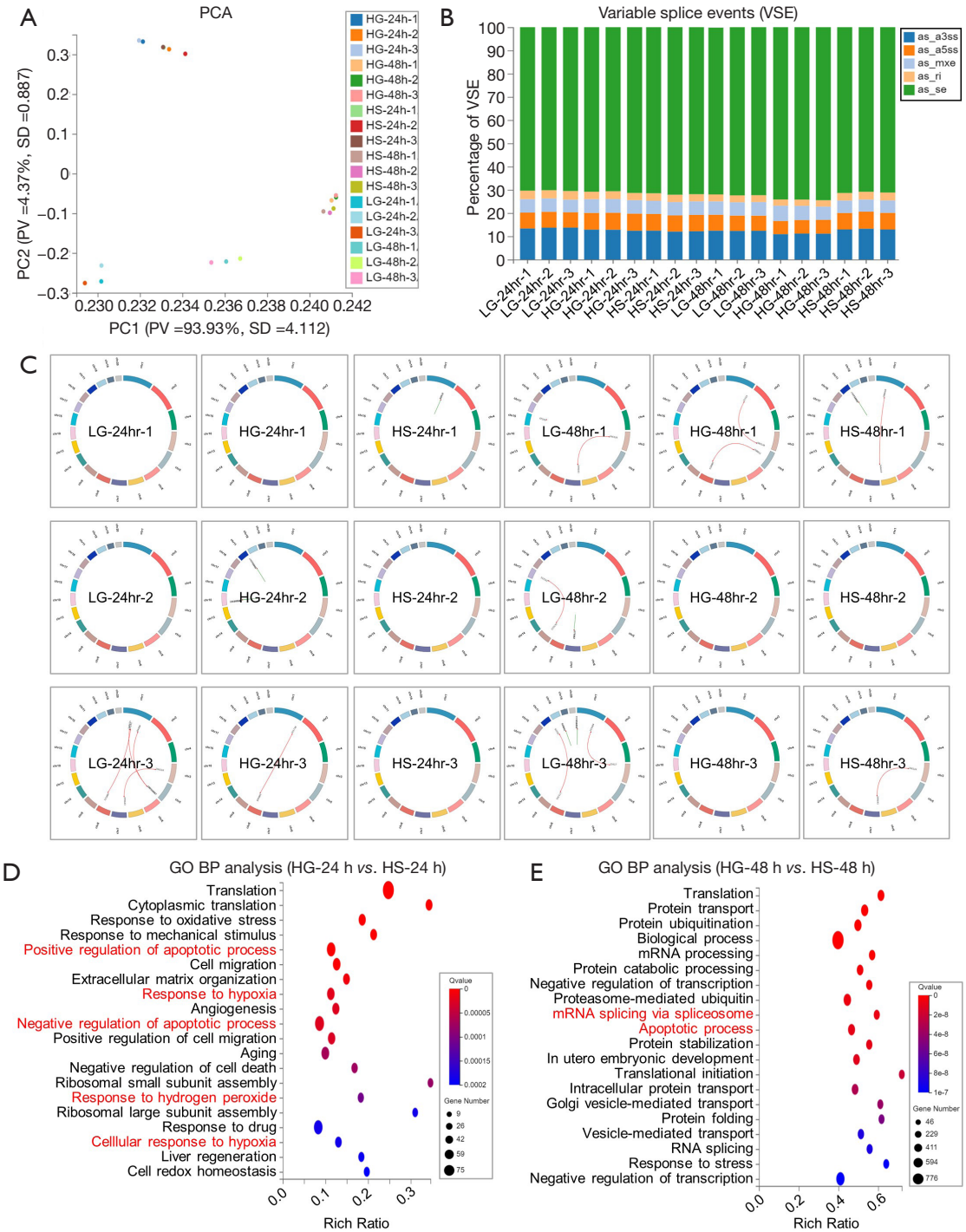

Figure 3 The signature of the genetic variation spectrum in the indicated groups. (A) PCA of the indicated groups (LG-24 h, HG-24 h, HS-24 h, LG-48 h, HG-48 h, HS-48 h). (B) The subtypes of VSE in the indicated groups (LG-24 h, HG-24 h, HS-24 h, LG-48 h, HG-48 h, HS-48 h). (C) The variations in the distribution of genes with different signatures of the genetic variation spectrum in the indicated groups (LG-24 h, HG-24 h, HS-24 h, LG-48 h, HG-48 h, HS-48 h) by Circos analysis. (D,E) GO analysis of the genes with different signatures of the genetic variation spectrum between HG-24 h and HS-24 h (D), or between HG-48 h and HS-48 h (E). PCA, principal component analysis; LG, low D-glucose; HG, high D-glucose; HS, high glucose and sulfuretted hydrogen; VSE, variable splice event; GO, gene ontology; PC, principal component; PV, percentage of variance; SD, standard deviation; BP, biological processes.

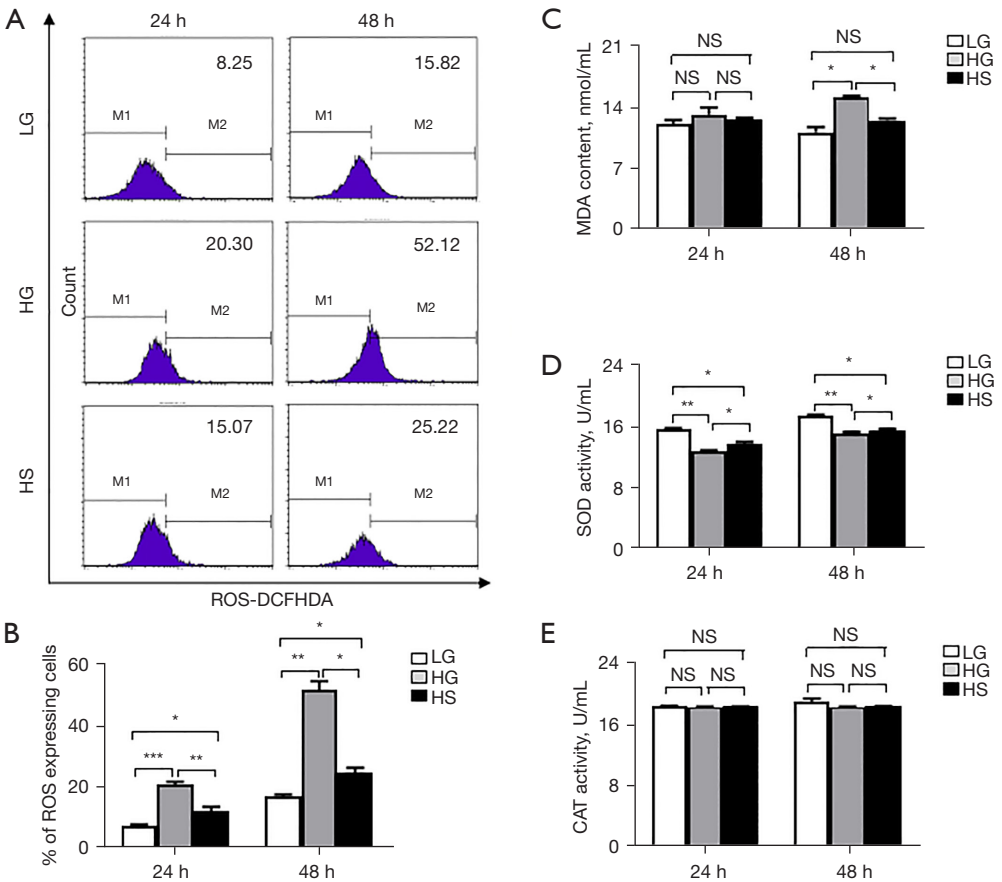

Figure 4 Sulfuretted hydrogen revealed antioxidative protective effects on podocytes. (A,B) Representative diagrams (A) and statistical analysis (B) of ROS in podocytes as determined by FCM. All data are shown as mean ± SD (n=3). *, P<0.05; **, P<0.01; ***, P<0.001. (C-E) Statistical analyses of MDA content (C), SOD activity (D), and CAT activity (E) in podocytes with the indicated treatments at 24 and 48 h. All data are shown as mean ± SEM (n=3). *, P<0.05; **, P<0.01; NS, not significant. ROS, reactive oxygen species; FCM, flow cytometry; MDA, malondialdehyde; SOD, superoxide dismutase; CAT, catalase; LG, low D-glucose; HG, high D-glucose; HS, high glucose and sulfuretted hydrogen.

AMPK/mTOR signaling in multiple physiological and pathological processes, such as cellular energy metabolism and drug resistance, as well as multiple aspects of cell vitality (e.g., apoptosis, proliferation, cell cycle) (18). We therefore compared the expression levels of phosphorylated p-AMPK and total AMPK in podocytes with the indicated treatments, and found that AMPK signaling was largely activated in the HS group compared to that in the HG group (*Figure 5A,5B*). Simultaneously, we further verified that sulfuretted hydrogen played a vital role in suppressing the phosphorylation of mTOR (*Figure 5A,5B*). Consistent with the protein bands, quantification of AMPK/mTOR signaling-associated proteins by gray scanning showed that the HG group manifested the highest levels of mTOR but the lowest level of p-AMPK, which could be significantly rescued by sulfuretted hydrogen (*Figure 5C-5F*).

Discussion

Podocytes, together with the basilar membrane of the glomerulus and glomerular endothelial cells, constitute the glomerular hemofiltration barrier and play a pivotal role in humoral homeostasis (18). The dysfunction of podocytes results in multiple renal diseases such as glomerular injury, human glomerular disease, and adriamycin-induced nephropathy (3,6). In this study, we demonstrated the important role and molecular mechanism of sulfuretted hydrogen in protecting podocytes from glucose-induced

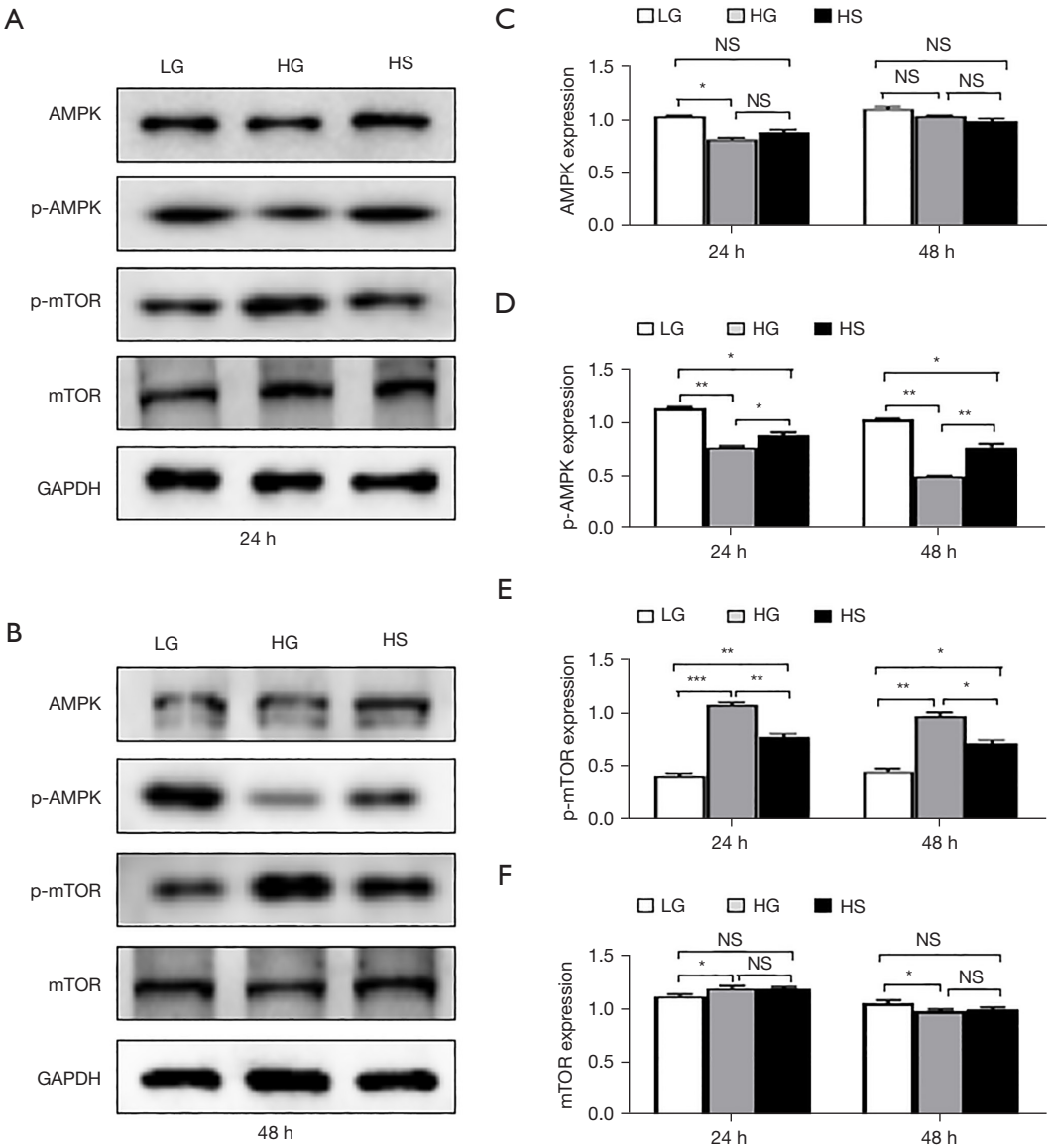

Figure 5 AMPK/mTOR signaling mediated the anti-apoptotic effect of sulfuretted hydrogen. (A,B) Western blotting analysis of AMPK, p-AMPK, p-mTOR, and mTOR proteins in podocytes with the indicated treatments at 24 h (A) and 48 h (B). GAPDH was the loading control. (C-F) Statistical analyses of AMPK (C), p-AMPK (D), p-mTOR (E), and mTOR (F) proteins in podocytes with the indicated treatments at 24 h and 48 h. All data are shown as mean ± SEM (n=3). *, P<0.05; **, P<0.01; ***, P<0.001; NS, not significant. LG, low D-glucose; HG, high D-glucose; HS, high glucose and sulfuretted hydrogen.

apoptosis. Generally, the pro-apoptotic effect of glucose stimulation could be largely rescued by sulfuretted hydrogen via an AMPK/mTOR-dependent approach. Collectively, our studies indicate the potential therapeutic effects of sulfuretted hydrogen on podocyte injury in a variety of glomerular diseases.

For decades, we and other investigators have been dedicated to decoding the etiology and pathogenesis of podocyte-associated human glomerular diseases (6,18-20). For instance, Chen and colleagues verified the soluble retinoic acid receptor responder protein 1 (RARRES1) as a critical inducer of podocyte apoptosis and glomerular disease progression (18). Zhong *et al.* demonstrated that Tyro3 could serve as a podocyte protective factor

in glomerular diseases, while another study suggested the deficiency of Sirt6 in the progression of proteinuria and podocyte injury by targeting Notch signaling (6,19). Meanwhile, Hua and colleagues verified that fatty acid translocase CD36 was associated with the increased uptake of fatty acid or ox-LDL in diabetic nephropathy kidney tissue (e.g., hepatocytes, macrophages, and proximal tubular epithelial cells), and was also involved in the fatty acid-induced apoptosis of podocytes via oxidative stress (e.g., translocation from the cytoplasm to the plasma membrane, accelerated lipid uptake and ROS production) (20). However, to our knowledge, the current progress in the field is scattered, and systematic and detailed information of podocyte-associated apoptosis in nephropathy is far from satisfactory. Thus, there is an urgent need to systematically and meticulously analyze pathological podocyte apoptosis and the underlying mechanism (6).

To this end, we used a glucose-induced podocyte apoptosis model to verify the protective effect of sulfuretted hydrogen, and uncovered the molecular mechanisms including antioxidative effects and AMPK/mTOR signaling-mediated anti-apoptosis. Notably, our study also revealed the potential influence of sulfuretted hydrogen stimulation on podocytes from the aspects of the transcriptome including DEGs and signatures of the genetic variation spectrum (e.g., the amount, distribution, and biological function of the VSEs). Additionally, current studies have also suggested the autophagy, genes (e.g., *Grem2*, *Sam68*, *Septin* 7) and noncoding RNA (e.g., lncRNA PVT1) preceded apoptosis and the inhibitory effect of PI3-kinase/Atg5 cascades in angiotensin II-induced podocyte injury (8,21-24). Additionally, sulfuretted hydrogen has been reported with protective effects against the TNF-α induced neuronal cell apoptosis in patients with spinal cord ischemia/reperfusion injury via modulating the miR-485-5p/TRADD axis, which further indicated the pharmacological effects and clinical application of sulfuretted hydrogen as well (9).

Notably, Daehn and colleagues indicated that scavenging of mitochondrial-targeted ROS in adjacent endothelial cells was sufficient for alleviating podocyte loss, segmental glomerulosclerosis, albuminuria, and renal failure (25). However, the detailed function and underlying mechanism of ROS in glucose-induced apoptosis of podocytes are largely unknown. Using RNA-Seq and accompanying bioinformatics analysis, we confirmed the involvement of hypoxia and metabolism-related BP, such as response to hypoxia and hydrogen peroxide, ribosomes, protein processing, and ferroptosis, in the glucose-induced apoptosis of podocytes. Moreover, we confirmed the protective effect of sulfuretted hydrogen on podocytes through anti-oxidative responses by the quantification of ROS and MDA content and SOD and CAT activity. Collectively, we demonstrated for the first time the glucose-induced apoptosis of podocytes and the protective effect of sulfuretted hydrogen on podocyte injury both at the cellular and molecular levels, which may provide new references for further understanding and decoding the etiology and treatment of podocyte-associated glomerular diseases in clinical practice.

Acknowledgments

We thank all the doctors and nurses in the Affiliated Hospital of Jiangxi University of Traditional Chinese Medicine for their technical support.
Funding: This work was supported by grants from Project funded by the National Natural Science Foundation of China (82060849, 81704052).

Footnote

Reporting Checklist: The authors have completed the MDAR reporting checklist. Available at https://dx.doi.org/10.21037/atm-21-5152

Data Sharing Statement: Available at https://dx.doi.org/10.21037/atm-21-5152

Conflicts of Interest: All authors have completed the ICMJE uniform disclosure form (available at https://dx.doi.org/10.21037/atm-21-5152). The authors have no conflicts of interest to declare.

Ethical Statement: The authors are accountable for all aspects of the work in ensuring that questions related to the accuracy or integrity of any part of the work are appropriately investigated and resolved.

References

1. Mundel P. Podocyte-targeted treatment for proteinuric kidney disease. Semin Nephrol 2016;36:459-62.
2. Tharaux PL, Huber TB. How many ways can a podocyte die? Semin Nephrol 2012;32:394-404.
3. Nagata M. Podocyte injury and its consequences. Kidney Int 2016;89:1221-30.
4. Raij L, Tian R, Wong JS, et al. Podocyte injury: the role of proteinuria, urinary plasminogen, and oxidative stress. Am J Physiol Renal Physiol 2016;311:F1308-17.
5. Egerman MA, Wong JS, Runxia T, et al. Plasminogenuria is associated with podocyte injury, edema, and kidney dysfunction in incident glomerular disease. FASEB J 2020;34:16191-204.
6. Liu M, Liang K, Zhen J, et al. Sirt6 deficiency exacerbates podocyte injury and proteinuria through targeting Notch signaling. Nat Commun 2017;8:413.
7. Dai H, Liu Q, Liu B. Research progress on mechanism of podocyte depletion in diabetic nephropathy. J Diabetes Res 2017;2017:2615286.
8. Liu DW, Zhang JH, Liu FX, et al. Silencing of long noncoding RNA PVT1 inhibits podocyte damage and apoptosis in diabetic nephropathy by upregulating FOXA1. Exp Mol Med 2019;51:1-15.
9. Chen Z, Zhang Z, Zhang D, et al. Hydrogen sulfide protects against TNF-α induced neuronal cell apoptosis through miR-485-5p/TRADD signaling. Biochem Biophys Res Commun 2016;478:1304-9.
10. Liu Y, Pan L, Jiang A, et al. Hydrogen sulfide upregulated lncRNA CasC7 to reduce neuronal cell apoptosis in spinal cord ischemia-reperfusion injury rat. Biomed Pharmacother 2018;98:856-62.
11. Liu Y, Zhao H, Qiang Y, et al. Effects of hydrogen sulfide on high glucose-induced glomerular podocyte injury in mice. Int J Clin Exp Pathol 2015;8:6814-20.
12. Li L, Jiang HK, Li YP, et al. Hydrogen sulfide protects spinal cord and induces autophagy via miR-30c in a rat model of spinal cord ischemia-reperfusion injury. J Biomed Sci 2015;22:50.
13. Hou H, Zhang L, Duan L, et al. Spatio-temporal metabolokinetics and efficacy of human placenta-derived mesenchymal stem/stromal cells on mice with refractory Crohn's-like enterocutaneous fistula. Stem Cell Rev Rep 2020;16:1292-304.
14. Zhao Q, Zhang L, Wei Y, et al. Systematic comparison of hUC-MSCs at various passages reveals the variations of signatures and therapeutic effect on acute graft-versus-host disease. Stem Cell Res Ther 2019;10:354.
15. Wei Y, Zhang L, Chi Y, et al. High-efficient generation of VCAM-1+ mesenchymal stem cells with multidimensional superiorities in signatures and efficacy on aplastic anaemia mice. Cell Prolif 2020;53:e12862.
16. Lu S, Ge M, Zheng Y, et al. CD106 is a novel mediator of bone marrow mesenchymal stem cells via NF-κB in the bone marrow failure of acquired aplastic anemia. Stem Cell Res Ther 2017;8:178.
17. Kayser S, Levis MJ. Clinical implications of molecular markers in acute myeloid leukemia. Eur J Haematol 2019;102:20-35.
18. Chen A, Feng Y, Lai H, et al. Soluble RARRES1 induces podocyte apoptosis to promote glomerular disease progression. J Clin Invest 2020;130:5523-35.
19. Zhong F, Chen Z, Zhang L, et al. Tyro3 is a podocyte protective factor in glomerular disease. JCI Insight 2018;3:123482.
20. Hua W, Huang HZ, Tan LT, et al. CD36 mediated fatty acid-induced podocyte apoptosis via oxidative stress. PLoS One 2015;10:e0127507.
21. Seong SB, Ha DS, Min SY, et al. Autophagy precedes apoptosis in angiotensin II-induced podocyte injury. Cell Physiol Biochem 2019;53:747-59.
22. Chen Y, Zhang L, Liu S, et al. Sam68 mediates high glucose-induced podocyte apoptosis through modulation of Bax/Bcl-2. Mol Med Rep 2019;20:3728-34.
23. Li R, Dong W, Zhang S, et al. Septin 7 mediates high glucose-induced podocyte apoptosis. Biochem Biophys Res Commun 2018;506:522-8.
24. Wen H, Kumar V, Mishra A, et al. Grem2 mediates podocyte apoptosis in high glucose milieu. Biochimie 2019;160:113-21.
25. Daehn I, Casalena G, Zhang T, et al. Endothelial mitochondrial oxidative stress determines podocyte depletion in segmental glomerulosclerosis. J Clin Invest 2014;124:1608-21.

(English Language Editor: C. Betlzar)

Cite this article as: Huang Y, Cheng J, Zhou Y, Zhang Y, Zhou S, Li Q, Peng L, Wang M, Song W, Wu G. Sulfuretted hydrogen ameliorates high dose glucose-induced podocyte apoptosis via orchestrating AMPK/mTOR cascade-mediated anti-apoptotic effects. Ann Transl Med 2021;9(20):1586. doi: 10.21037/atm-21-5152

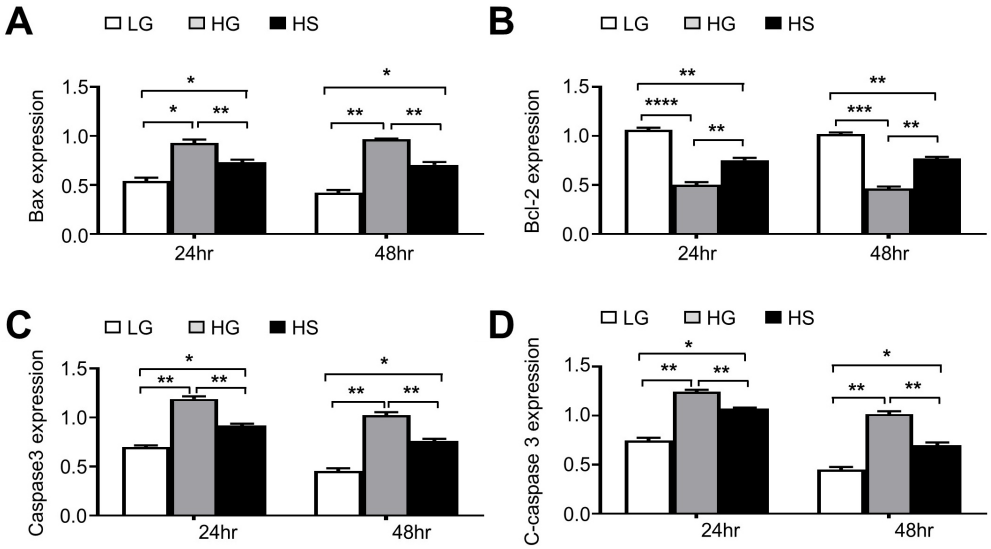

Figure S1 The statistical graph of western blot (A-D) The statistical graph of western blot including Bax (A), Bcl-2 (B), caspase 3 (C), c-caspase 3 (D) in the indicated groups (LG, HG, HS) at indicated time points (24 and 48 h). All data were shown as mean ± SEM (n=3 independent experiments). *, P<0.05; **, P<0.01; ***, P<0.001. LG, low D-glucose; HG, high D-glucose; HS, high glucose and sulfuretted hydrogen.

Table S1 The information of the indicated antibodies

Antibody	Cat. no.	Source
Annexin-V/PI kit	MA0220	Meilun Bio
Hoechst 33258	C1018	Beyotime
Caspase 3	BC3830	Solarbio
ROS-DCFHDA	MA0219	Meilun Bio
Bax	50599-2-Ig	Proteintech
Bcl-2	26593-1-AP	Proteintech
Caspase 3	19677-1-AP	Proteintech
C-caspase 3	#9661	Cell signaling
AMPK	66536-1-Ig	Proteintech
p-AMPK	bs-8813R	Bioss
mTOR	5536S	Sino biological
p-mTOR	66888-1-Ig	Proteintech
GAPDH	60004-I-Ig	Proteintech

https://dx.doi.org/10.21037/atm-21-5152